International Journal of Fatigue 70 (2015) 278–288

Contents lists available at ScienceDirect

International Journal of Fatigue

journal homepage: www.elsevier.com/locate/ijfatigue

High and low cycle fatigue behavior of linear friction welded Ti–6Al–4V

J.C. Stinville [a,*], F. Bridier [a,1], D. Ponsen [a], P. Wanjara [b], P. Bocher [a]

[a] Department of Mechanical Engineering, École de technologie supérieure, Montréal, Canada
[b] National Research Council Canada, Aerospace, Montréal, Canada

ARTICLE INFO

Article history:
Received 8 July 2014
Received in revised form 30 September 2014
Accepted 1 October 2014
Available online 12 October 2014

Keywords:
Friction welding
Fatigue properties
Ti alloys
Digital image correlation
Electron backscatter diffraction

ABSTRACT

Linear friction welded Ti–6Al–4V was investigated in fatigue at various stress amplitudes ranging from the high cycle fatigue (HCF) to the low cycle fatigue (LCF) regime. The base material was composed of hot-rolled Ti–6Al–4V plate that presented a strong crystallographic texture. The welds were characterized in terms of microstructure using electron backscatter diffraction and hardness measurements. The microstructural gradients across the weld zone and thermomechanically affected zone of the linear friction welds are discussed in terms of the crystallographic texture, grain shape and hardness levels, relative to the parent material. The location of crack nucleation under fatigue loading was analyzed relative to the local microstructural features and hardness gradients. Though crack nucleation was not observed within the weld or thermomechanically affected zones, its occurrence within the base material in LCF appears to be affected by the welding process. In particular, by performing high resolution digital image correlation during LCF, the crack nucleation site was related to the local accumulation of plastic deformation in the vicinity of the linear friction weld.

1. Introduction

Linear friction welding (LFW) involves solid-state joining of materials through the relative linear reciprocating motion of one component against a fixed stationary component under axial compressive forces [1–3], as illustrated in Fig. 1. For Ti–6Al–4V, Vairis and Frost [3] have identified that four distinct phases occur during the process, namely the initial phase, the transition phase, the equilibrium phase and the forging phase. The friction between the parts generates heat, which together with the applied force results in a consolidated joint seam with a limited plastically or thermomechanically affected zone (TMAZ). Linear friction welds in titanium alloys exhibit good mechanical properties [4–6] as compared to other joining techniques such as laser welding [7], electron beam welding or inertia friction welding [8].

Aeroengine industries drive most of the LFW development in order to build integrated bladed rotors, for which the disk and blades are integrated as a monolithic component. Bladed disks, commonly termed blisks, may (1) provide considerable weight savings through elaboration of the design and manufacturing, (2) improve in-service performance, (3) offer interesting repair solutions over conventional slotted blade-disk assemblies and (4) avoid fretting issues by eliminating the high frequency oscillatory slip in the attachment area of the blade to disc. For aeroengine applications, LFW is most propitious for titanium alloys, which commonly compose the low-pressure stages of the compressor, where the large size of the blades highly motivates the development of such a joining technology.

During LFW of titanium alloys, extensive deformation at high temperatures occurs and generates significant changes in the microstructure of the parent material. Previous studies [9–16] report three dissimilar microstructural zones across the weldment, which are the weld zone, the TMAZ and the parent material. Specifically, in the weld zone of alpha–beta (α–β) titanium alloys, exposure to temperatures above the β-transus combined with high strain rates and strains induce the formation of fine recrystallized β grains that transform during rapid cooling after welding to a martensitic–Widmanstätten α microstructure. In the TMAZ, elongated α grains with interspersed metastable β phase are observed. Interestingly, LFW can also be used to weld two dissimilar kinds of alloys [17] or the same alloy, but with dissimilar microstructures [18].

In the present study, welds between dissimilar textured Ti–6Al–4V specimens were produced and characterized, in order to simulate the potential difference in microstructure and fatigue strength across a weld between a blade and a disk. In particular, compressor blades and disks are exposed to different fatigue regimes and it was deliberated that a tailored texture for each sub-component could help

* Corresponding author. Tel.: +1 805 893 4362.
E-mail address: stinville@engineering.ucsb.edu (J.C. Stinville).
[1] Present address: DCNS Research, Indret, 44620 La Montagne, France.

http://dx.doi.org/10.1016/j.ijfatigue.2014.10.002
0142-1123/

optimize fatigue performance by, for example, having the blade and disk consisting of optimal textures suited to their particular fatigue regime. Thus, a large range of stress levels was considered in this work, since the blades are typically exposed to HCF and the disk to both LCF and HCF. Accordingly, the fatigue properties at room temperature of a dissimilar textured Ti–6Al–4V linear friction welded (LFWed) assembly are reported here.

2. Experimental procedures

2.1. Material and welding

A typical titanium alloy used for the low pressure compressors and the first stage of the high pressure compressors is Ti–6Al–4V. As such, hot rolled Ti–6Al–4V material was procured in bar form with a nominal chemical composition in wt.% of 6% Al, 4% V, 0.19% Fe, 0.15% O, 0.06% C, 0.04% N, and 0.01% H. Coupons or blocks (L: 35 mm, W: 13 mm, and H: 25 mm) for LFW were machined with special attention given to their orientation in the as-received rolled plate of Ti–6Al–4V. Specifically, 50% of the blocks were machined with their length (L in the schematic illustrated in Fig. 1) along the rolling direction (RD) and the other 50% with their length along the transverse direction (TD) of the hot-rolled bar. LFW was performed between these two coupon types, as shown by the schematic representation given in Fig. 1. It is noteworthy that the as-received material was composed of more than 95 vol.% hexagonal close-packed (hcp) α-phase and less than 5 vol.% body-centered cubic (bcc) β-phase. The microstructure was characterized by globular primary α_p-phase nodules (about 15 μm in diameter) and secondary α_s-plates (about 1 μm thick) embedded in the prior β matrix, as apparent in Fig. 2d and e.

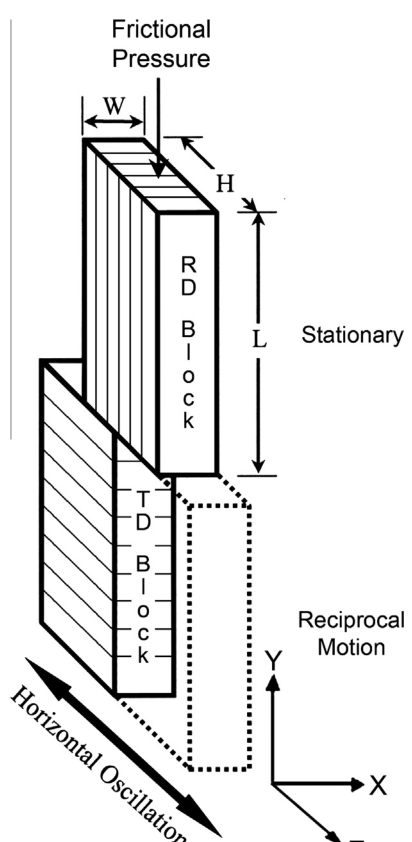

Fig. 1. A schematic side view of the workpiece showing the linear friction welding process on two Ti–6Al–4V blocks. The lines demarcated on the two weld blocks (RD and TD) present the rolling direction of the as-received Ti–6Al–4V rolled plate.

LFW was performed at ambient temperature under prevailing atmospheric conditions using a MTS Linear Friction Welding Process Development System. The facility is comprised of two hydraulic actuators. The in-plane actuator oscillates the lower work piece horizontally. The forge actuator applies a downward load through the top stationary work piece (Fig. 1). The parameters for LFW consist of the oscillation frequency, amplitude, axial shortening and pressure. Typically for LFW of titanium alloys the process operation range is relatively wide for the frequency (15–100 Hz), amplitude (±0.2–0.5 mm) and pressure (30–150 MPa). In this work with the oscillation frequency, amplitude and axial shortening being fixed, two arbitrary frictional pressures of P and 2P were used during LFW of the blocks. (Other experimental details can be found in [9]).

2.2. Microstructure characterization

Crystallographic and morphologic textures were obtained from electron backscatter diffraction (EBSD) measurements using a HITACHI SU-70 field emission gun scanning electron microscope (SEM) with an orientation imaging microscopy system (HKL – Channel 5). Specimens were systematically and carefully aligned along one of the axes of the microscope stage. Thereby, the three-dimensional local crystalline orientation of the hcp α phase could be related to the macroscopic axes of the specimens. EBSD scans with various spatial resolution relative to the microstructural fineness were performed with a square grid at an acceleration voltage of 20 kV and a beam current of typically about 0.2 nA. It is noteworthy that in the inverse pole figure map, crystallographic orientation is given relative to the direction along the length of the blocks (Y), which corresponds to the direction normal to the weld, i.e., the subsequent loading axis of mechanical fatigue tests. Acquisition of the crystallographic orientation of the β-phase was not conducted, with due consideration of the low fraction of this phase and the relative significance in view of the measurement error. Evolution of the texture in the weld is described using the density of pole figures (half width: 10°; cluster size: 5°) given as multiples of uniform distribution (mud). The Kearns factors Fx, Fy and Fz were used to numerically describe the evolution of the crystallographic texture across the weld relative to the macroscopic axis X, Y and Z [19]. Kearns factors of 1/3 indicate a random orientation distribution along the three directions X, Y and Z.

2.3. Hardness measurements

The hardness across the weld region at the axial centerline was measured using a 100 g load applied for 30 s with a Vickers micro hardness tester. The indent interval was 0.1 mm and the minimum test point separation distance was at least three times the diagonal measurement of the indent. It is noteworthy that the hardness values were determined from the high accuracy measurements of the diagonals of the indents using secondary electron microscopy. Several hardness profiles across the weldment were performed in the middle of the specimen, where the TMAZ was narrowest.

2.4. Fatigue tests

Cylindrical specimens (4 mm diameter in the gauge section and gauge length of 13 mm) were machined from the welded specimens, in such a way that the weld was located in the middle of the gauge length. The specimens were mechanically polished to a surface finish of 1 μm. Fatigue tests were carried out at room temperature and in stress control mode on a servo-hydraulic closed-loop MTS 810 frame. A stress ratio of $R = 0.1$ and a sinusoidal waveform at a frequency of 1 Hz were selected for testing. A MTS 10 mm base extensometer was used to measure the strain.